Asian Journal of Andrology (2020) 22, 578–582
www.asiaandro.com; www.ajandrology.com

Open Access

ORIGINAL ARTICLE

Sperm Biology

Relationship of sperm plasma membrane and acrosomal integrities with sperm morphometry in *Bos taurus*

Inmaculada Palacín[1], Pilar Santolaria[1], Carlos Alquezar-Baeta[2], Carles Soler[3], Miguel A Silvestre[3], Jesús Yániz[1]

To date, sperm morphometric studies have assessed whole sperm populations without considering sperm function. The aim of this study was to evaluate the relationship of sperm membrane and acrosomal integrity with sperm morphometry in liquid semen samples collected from bulls. To this end, sperm morphometry was performed on cryopreserved semen samples from 16 bulls by a combination of fluorescent dyes, including Hoechst 33343, carboxyfluorescein diacetate, and propidium iodide. This allowed discrimination of different subpopulations on the basis of sperm membrane and acrosomal integrity and analysis of the morphometrics of the sperm head, nucleus, and acrosome using a specific plug-in module created on ImageJ. Acrosomal integrity was related to sperm morphometry as the heads of spermatozoa with a damaged acrosome were significantly smaller than those with a normal acrosome ($P < 0.001$). In the case of spermatozoa with an intact acrosome, those with a damaged plasma membrane had a larger sperm head and acrosome than spermatozoa with an intact plasma membrane ($P < 0.001$). No significant differences in the sperm head size were observed between sperm subpopulations without an acrosome or in the nuclear sperm morphometry of the different subpopulations. There was a positive correlation between the sperm motility values of the samples and the morphometric parameters for intact spermatozoa. These correlations were particularly strong for the morphometric parameters of the sperm acrosome. We conclude that there are clear differences in the sperm morphometry depending on the status of the sperm membrane and acrosome and this should be considered when performing this kind of analysis.

Asian Journal of Andrology (2020) **22**, 578–582; doi: 10.4103/aja.aja_2_20; published online: 21 April 2020

Keywords: *Bos taurus*; fluorescence microscopy; image analysis; sperm morphometry; sperm quality

INTRODUCTION

Sperm morphology analysis is recognized as a fundamental component of the spermiogram. Evidence from different species has shown that the presence of poor sperm morphology may determine low fertility rates.[1] Sperm morphometry is linked to the genetic and DNA characteristics of the cell.[2] However, the most common protocols, including sample smearing, air-drying, fixation, and staining, introduce artifacts and alter sperm morphology.[3–6] In recent years, several studies have described new techniques for analyzing sperm morphology from wet preparations to avoid introducing air-drying-induced artifacts. These include the use of phase-contrast[4,7–11] and fluorescence microscopy.[5,6] These techniques should preferably be combined with a pressure method when preparing the slides, such as the Trumorph® (PROISER, Paterna, Spain), to avoid trapping spermatozoa in different focal planes and to ensure that the heads are aligned in a single plane.[11]

Despite progress, current sperm morphometric methods are based on the study of the whole sperm population without considering potential differences between live and dead cells or those with intact and damaged acrosomes. This may lead to misinterpretations as, for example, differences in the sperm morphometry between males may be erroneously attributed to factors other than simply poor sperm quality. In a recent study, we described a new fluorescence method that clearly identifies whether bull spermatozoa have an intact or damaged plasma membrane and acrosome.[12] The aim of the present work was to use this method to perform a detailed morphometric study of the different sperm subpopulations present in the liquid semen samples from bulls.

MATERIALS AND METHODS

Semen collection and processing

All animals were handled according to the procedures approved by the University of Zaragoza Ethics Committee (Zaragoza, Spain), and the research was performed in accordance with the Spanish Policy for Animal Protection (RD53/2013), which conforms to European Union Directive 86/609 regarding the protection of animals used in scientific experiments. The study analyzed cryopreserved semen samples collected from 16 commercial Holstein bulls. The ejaculate was then extended in BullXcell (IMV Technologies, Humeco, Huesca, Spain) to a final concentration of 23×10^6 sperm per 0.25 ml semen straw (IMV Technologies). Straws were cooled to 4°C over 3 h and then frozen to −140°C as follows: −5°C per min from +4°C to −10°C, −40°C

[1]BIOFITER Research Group, Environmental Sciences Institute (IUCA), Department of Animal Production and Food Sciences, University of Zaragoza, Huesca 22071, Spain; [2]Department of Computer Science, University of Zaragoza, Zaragoza 50018, Spain; [3]Department of Cellular Biology, Functional Biology and Physical Anthropology, University of Valencia, Burjassot 46100, Spain.
Correspondence: Dr. J Yániz (jyaniz@unizar.es)
Received: 25 June 2019; Accepted: 03 December 2019

per min from −10°C to −100°C, and thereafter −20°C per min from −100°C to −140°C in a programmable freezer (IMV Technologies), followed by submersion and storage in liquid nitrogen at −196°C until use. Before use, straws were thawed in a water bath for 1 min at 37°C and processed to study the sperm quality.

Sperm motility assessment by computer-assisted sperm analysis (CASA-Mot)

Sperm motility was measured after placing a diluted semen sample in a prewarmed Makler (Sefi-Medical Instruments Ltd., Haifa, Israel) chamber.[13] For this purpose, a computer-assisted sperm analyzer (CASA-Mot; ISAS®, version 1.0; PROISER) and an Olympus BX40 (Olympus, Optical Co., Tokyo, Japan) microscope equipped with a negative phase-contrast 10× objective and heated stage set at 37°C were used. The motility variables measured included the curvilinear velocity (VCL, μm s^{-1}), straight line velocity (VSL, μm s^{-1}), average path velocity (VAP, μm s^{-1}), sperm linearity (LIN), straightness (STR), amplitude of lateral sperm head displacement (ALH, μm), and beat cross-frequency (BCF, Hz).[13]

Fluorescence imaging and computer-assisted sperm morphometry analysis (CASA-Morph)

Samples were labeled with the ISAS®3Fun kit (PROISER) as described.[12] The labeling mix included three fluorochromes: propidium iodide, Hoechst 33343, and carboxyfluorescein diacetate (CFDA); therefore, plasma membrane and acrosomal integrity could be assessed simultaneously in wet samples. A 4-μl aliquot of the fluorochrome combination from the kit was mixed with 40 μl of the sample and incubated in a water bath for 5 min at 37°C. Then, 3 μl of the labeled and diluted sample was placed on a prewarmed slide, covered, and pressed with the Trumorph® system (PROISER).[11] Fluorescent microspheres (PS-Speck Blue 360/440, Green 505/515, and Red 633/660 Microscope Image Calibration Kit, Molecular Probes, Madrid, Spain) were mounted on separate slides and used as fluorescence intensity standards.

An epifluorescence microscope (DM4500B, Leica, Wetzlar, Germany), equipped with a warmed stage, a 63× plan apochromatic oil immersion objective, standard blue/green/red (B/G/R, excitation: 420–430, 495–515, 570–620 nm), blue (A, excitation: 340–380 nm), green (I3, excitation: 450–490 nm), and red (N2, excitation: 515–560 nm) filter sets, was used to obtain digital images of the fluorescence-labeled sperm. Images were captured using a Canon EOS 600D Digital Camera controlled with EOS Utility software (Canon Inc., Tokyo, Japan).

Four image sequences were captured from each microscope field using different filter sets: (1) a B/G/R filter for the whole sperm head; (2) a G filter for the acrosome; (3) a B filter for the nuclei of live spermatozoa; and (4) a R filter for the nuclei of dead spermatozoa.

Sperm were grouped into four sperm subpopulations (**Figure 1**): (a) those with an intact acrosome and plasma membrane (IAIM); (b) those with an intact acrosome and a damaged plasma membrane (IADM); (c) those with a damaged acrosome and an intact plasma membrane (DAIM); and (d) those with a damaged acrosome and plasma membrane (DADM).

Sperm head, acrosome, and nucleus morphometry from each sperm of the different subpopulations were automatically analyzed in each image sequence (**Figure 1**) using ImageJ open software (version 1.45e, available at http://rsbweb.nih.gov/ij/download.html) and a new sperm morphometric plug-in module developed specifically for this study (available at https://github.com/calquezar/Biofiter_morph).

Four primary morphometric parameters and four derived parameters (secondary parameters) were measured for each sperm head and nucleus. Primary parameters included area (A, μm^2, the sum of all pixels contained within the boundary), perimeter (P, μm, the sum of external boundaries), length (L, μm) and width (W, μm), and the largest and smallest Feret diameters. Secondary parameters included ellipticity (L/W), rugosity ($4\pi A/P^2$), elongation ([L − W]/[L + W]), and regularity ($\pi LW/4A$). The area of the head occupied by the acrosome (%) and the acrosomal area (μm^2) were also measured in IAIM and IADM subpopulations. At least 200 sperms per sample were analyzed. The same person carried out image capture and morphometric analysis on all samples.

Statistical analyses

We analyzed the sperm morphometry of 5408 spermatozoa. The values obtained were expressed as mean ± standard deviation (s.d.). Statistical analyses were performed using the SPSS package, version 15.0 (SPSS, Inc., Chicago, IL, USA). Distribution normality and the homogeneity of variance of the median score for each data set were checked using the Kolmogorov–Smirnov and Levene tests, respectively.[14] For normally distributed variables, differences in the sperm morphometric parameters were evaluated by analysis of variance (ANOVA), including the bull as a random variable, followed by the Tukey's *post hoc* test. For nonnormally distributed populations, the Kruskal–Wallis test, followed by the Mann–Whitney *post hoc* test, was used to compare the sperm morphometric parameters. Statistical significance was set at $P < 0.05$. Correlation analyses between morphometric measurements of IAIM ($n = 2397$) and sample motility parameters were performed using Pearson's (when variables were normally distributed) and Spearman's (when variables were nonnormally distributed) correlation coefficients. A Bonferroni correction is applied for all calculations to account for the multiple comparisons. The critical level was modified from $P < 0.05$ to $P < 0.004$ by Bonferroni correction.

RESULTS

Table 1 presents the primary morphometric parameter values for the different sperm subpopulations. Spermatozoa with a damaged acrosome (DAIM and DADM) had significantly smaller head dimensions than those with an intact acrosome, with mean differences in the sperm head area of 6.9% between IAIM and DAIM and 10.9% between IADM and DADM. Spermatozoa with an intact acrosome and a damaged plasma membrane (IADM) had significantly larger heads than the other subpopulations. These differences involved a 4.0% increase in the sperm head area in IADM with respect to the IAIM subpopulation. IADM spermatozoa also had an increase in acrosomal area compared with the IAIM subpopulation, although both subpopulations had a similar percentage of acrosomal head coverage. There were no significant differences in sperm head size between the two subpopulations with damaged acrosomes (DAIM and DADM) or in the nuclear sperm morphometry for all four subpopulations.

Table 2 shows the secondary morphometric parameter values for each of the sperm subpopulations. Head ellipticity and elongation were significantly higher and head regularity was lower in the subpopulations with damaged acrosomes (DAIM and DADM) than those with intact acrosomes (IAIM and IADM). The nuclei of the different subpopulations did not present any clear differences with respect to secondary morphometry parameter values.

There was a positive correlation between several CASA-Mot motility values of the samples and the primary morphometric parameters for the sperm head and acrosome of the IAIM subpopulation (**Table 3**). These correlations were particularly strong for the morphometric parameters associated with the sperm acrosome.

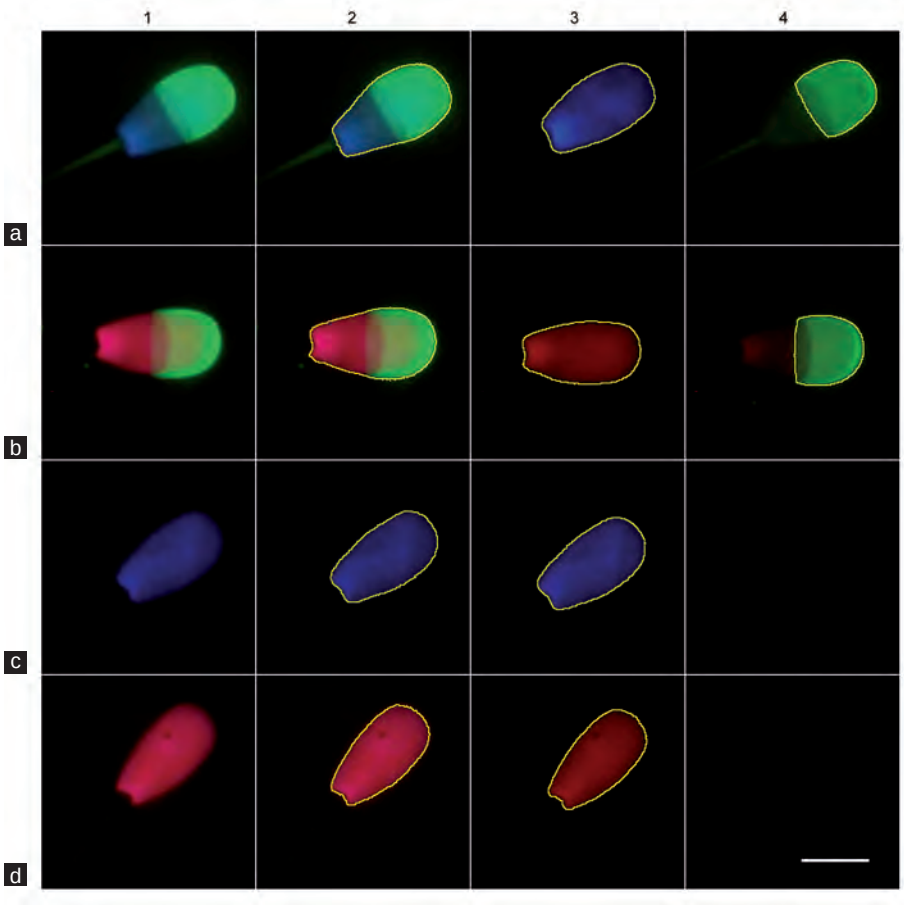

Figure 1: Bull sperm subpopulations stained with ISAS®3Fun (1), and their mask obtained after processing with an ImageJ plug-in module (2–4). Spermatozoa with (**a**) intact acrosome and membrane; (**b**) intact acrosome and damaged membrane; (**c**) damaged acrosome and intact membrane; and (**d**) damaged acrosome and membrane. The software automatically analyzes the sperm head (2), nucleus (3), and acrosome (4) and provides morphometric measurements. Scale bar= 5 μm.

Table 1: Primary sperm morphometric parameter values (mean±standard deviation) in four fluorescent subpopulations detected by using ISAS®3Fun

Sperm subpopulation	*IAIM*	*IADM*	*DAIM*	*DADM*	*P*
Number	2397	404	878	1729	
Head					
Area (μm²)	38.05±2.28[a]	40.15±2.30[b]	35.27±2.19[c]	35.13±1.99[c]	0.001
Perimeter (μm)	25.35±0.85[a]	26.27±0.87[b]	24.43±0.85[c]	24.60±0.83[d]	0.001
Length (μm)	9.38±0.36[a]	9.69±0.37[b]	9.08±0.37[c]	9.12±0.36[d]	0.001
Width (μm)	5.25±0.24[a]	5.47±0.25[b]	4.91±0.20[c]	4.86±0.19[d]	0.001
Nucleus					
Area (μm²)	35.11±2.16[a]	34.81±2.30[b]	34.84±2.23[b]	34.57±2.06[c]	0.001
Perimeter (μm)	24.12±0.78	24.17±0.86	24.00±0.82	24.10±0.80	0.129
Length (μm)	9.01±0.35	9.05±0.38	8.97±0.36	9.04±0.37	0.238
Width (μm)	4.87±0.21[a]	4.82±0.21[b]	4.85±0.20[a]	4.80±0.19[c]	0.001
Acrosome					
Area (μm²)	22.50±1.41[a]	23.79±1.73[b]	No acrosome	No acrosome	0.001
Percentage (%)	59.21±3.07	59.29±3.36			0.823

IAIM: spermatozoa with an intact acrosome and membrane; IADM: spermatozoa with an intact acrosome and a damaged membrane; DAIM: spermatozoa with a damaged acrosome and an intact membrane; DADM: spermatozoa with a damaged acrosome and membrane. [a-d]Values with different superscript letters in the same row are significantly different (P<0.001)

DISCUSSION

Up until now, sperm morphometry protocols have assessed whole sperm populations without considering sperm integrity. This may lead to misinterpretations if this factor has a similar or greater influence as other factors that affect sperm morphometry. The fluorescence combination used in the present work permitted, for the first time, a detailed study of the sperm morphometry of the different subpopulations present in a liquid semen sample, which were classified according to the sperm plasma membrane and acrosome integrity. This has provided relevant information about the influence of sperm function on sperm head morphometry.

Table 2: Secondary sperm morphometric parameter values (mean±standard deviation) in four fluorescent subpopulations detected by using ISAS®3Fun

Sperm subpopulation	*IAIM*	*IADM*	*DAIM*	*DADM*	*P*
Head					
Ellipticity	1.790±0.09[a]	1.775±0.10[b]	1.853±0.10[c]	1.882±0.11[d]	0.001
Roughness	0.744±0.02[a]	0.731±0.02[b]	0.742±0.02[a]	0.730±0.03[b]	0.001
Elongation	0.282±0.02[a]	0.278±0.03[b]	0.298±0.02[c]	0.305±0.03[d]	0.001
Regularity	1.017±0.02[a]	1.036±0.02[b]	0.992±0.02[c]	0.990±0.01[d]	0.001
Nucleus					
Ellipticity	1.852±0.10[a]	1.880±0.11[b]	1.850±0.10[a]	1.886±0.11[b]	0.001
Roughness	0.758±0.02[a]	0.748±0.02[b]	0.760±0.02[a]	0.748±0.02[b]	0.001
Elongation	0.298±0.02[a]	0.305±0.03[b]	0.298±0.02[a]	0.306±0.03[b]	0.001
Regularity	0.982±0.01[a]	0.986±0.01[b]	0.982±0.01[a]	0.987±0.02[b]	0.001

IAIM: spermatozoa with an intact acrosome and membrane; IADM: spermatozoa with an intact acrosome and a damaged membrane; DAIM: spermatozoa with a damaged acrosome and an intact membrane; DADM: spermatozoa with a damaged acrosome and membrane. [a-d]Values with different superscript letters in the same row are significantly different ($P<0.001$)

Table 3: Correlations coefficients (*r*) from Pearson's and Spearman's correlation analysis between morphometric measurements of spermatozoa with an intact acrosome and membrane and sample motility parameters

Sperm parameter	*Head*				*Acrosome*	
	Area (μm²)	*P*	*Perimeter (μm)*	*P*	*Area (μm²)*	*P*
VCL (μm s^{-1})					0.735	0.001
VSL (μm s^{-1})					0.779	0.001
VAP (μm s^{-1})					0.732	0.001
STR (%)	0.677	0.003	0.818	0.000	0.744	0.001
ALH (μm)					0.735	0.001

VCL: curvilinear velocity; VSL: straight line velocity; VAP: average path velocity; STR: straightness; ALH: lateral head displacement

The literature contains very few studies into the morphometric differences between spermatozoa on the basis of their plasma membrane and acrosome integrity. In a study using phase-contrast microscopy, Marco-Jimenez *et al*.[7] observed that spermatozoa with a damaged plasma membrane had a smaller head than those with an intact plasma membrane. These differences were attributed to the partial loss of cellular content due to plasma membrane rupture. However, the main constituent of the sperm head is chromatin,[15,16] and the results of our study revealed that spermatozoa with damaged acrosomes had similar sperm morphometry regardless of their plasma membrane status (DAIM *vs* DADM). Furthermore, the morphometric parameters of the sperm nuclei in these subpopulations are quite similar to those of the whole sperm head, which confirms that the plasma membrane only has a minor impact on sperm head morphometry.[17]

In artiodactyls, traditional staining protocols have failed to provide enough contrast to study acrosomal sperm morphometry. We have previously developed different approaches to circumvent this obstacle, including the use of contrast optics[18] or fluorochrome combinations in the semen smears.[19,20] In these studies, we observed that the highest variability in sperm morphometry between species,[19] and even between animals within species,[20] was evident in parameters related to the sperm acrosome. The study of the sperm morphometry of the acrosome may have functional interest as, in human, Menkveld *et al*.[21] found strong correlations between normal acrosomal morphology and IVF rates. Later, the same group related the acrosomal size to susceptibility to cell death and nonphysiological acrosomal loss.[22]

The fluorochrome combination used in the present study allows the differential staining of sperm head components in the liquid samples, and therefore, we revealed new evidence about the variability of sperm morphometry with respect to the acrosome. This structure is responsible for significant variations in sperm morphometry, as the loss of the acrosome caused a large reduction in the sperm head size. Furthermore, the acrosome of sperm with a damaged plasma membrane demonstrated a clear increase in the acrosomal area. This increase may be associated with a higher percentage of acrosome-reacted cells in the sperm subpopulation with a damaged plasma membrane. The acrosome loses structure during the acrosome reaction; hence, in some cases, the acrosome has a considerably larger surface over sperm anterior end.[1]

As in previous studies,[19,20] the sperm head was larger than the nucleus when the acrosome was present. This may be attributed to the fact that the free border of the acrosome was also stained with the ISAS®3Fun fluorochrome combination.[19]

There are indications that changes in head/nuclear morphometry may be related to chromatin status.[16,23] Given that sperm with a damaged plasma membrane apparently suffers more DNA fragmentation,[24] we should not rule out a possible association between sperm nuclear morphometry and plasma membrane status. In the present study, however, no significant differences in sperm nuclear morphometry were observed between sperm with an intact or damaged plasma membrane.

There was a positive correlation between the samples CASA-Mot parameters and the morphometric parameters for intact sperm. To the best of our knowledge, this is the first time that these correlations have been described for the morphometric parameters of sperm acrosome. We selected the IAIM sperm to study this association because spermatozoa with a damaged plasma membrane are immotile and those with a normal membrane and damaged acrosome show reduced motility.[12] Previous studies have also described correlations between the morphometry of all spermatozoa and sperm motility.[25,26]

The morphometric analyses in the current study were performed with the aid of a specific plug-in module developed on ImageJ. This was adapted to perform the analysis required in this work on images obtained with different fluorescence filters for each sperm. However, in practice, it may also be applied to the same image but by opening different copies for each channel. This can provide morphometric information for the whole sperm head and the acrosome, but not for the nucleus. In the future, we hope to integrate this function in the OpenCASA software recently developed by our research group (IUCA, University of Zaragoza, Zaragoza, Spain).[27]

CONCLUSIONS

The new sperm morphometry method described in this article can be used to conduct a detailed study of the sperm head components in different sperm subpopulations present in the liquid semen samples from bulls. The simultaneous morphometric assessment of sperm head, nucleus, and acrosome has revealed clear differences in function of

sperm membrane and acrosomal status, which should be considered when performing this kind of analysis.

AUTHOR CONTRIBUTIONS

IP and JY designed the experiments. IP, PS, and JY performed the experiments. IP, PS, CS, MAS, and JY analyzed the data. CAB designed the ImageJ plugin. IP and JY wrote the manuscript together with input from PS, CAB, CS, and MAS. All authors read and approved the final manuscript.

COMPETING INTERESTS

All authors declare no competing interests.

ACKNOWLEDGMENTS

This work was supported by the Spanish Ministry of Economy and Finance (MINECO) (grant AGL2017-85030-R), the European Territorial Cooperation Operational Program – Spain, France, and Andorra Area 2014–20 (Program DietaPYR2 EFA144/16), and the DGA-FSE (grant A07_17R). We would like to acknowledge the use of the Research Support Service-SAI, University of Zaragoza.

REFERENCES

1 Yaniz JL, Soler C, Santolaria P. Computer assisted sperm morphometry in mammals: a review. *Anim Reprod Sci* 2015; 156: 1–12.
2 Thurston LM, Watson PF, Mileham AJ, Holt WV. Morphologically distinct sperm subpopulations defined by Fourier shape descriptors in fresh ejaculates correlate with variation in boar semen quality following cryopreservation. *J Androl* 2001; 22: 382–94.
3 Katz DF, Overstreet JW, Samuels SJ, Niswander PW, Bloom TD, *et al*. Morphometric analysis of spermatozoa in the assessment of human male-fertility. *J Androl* 1986; 7: 203–10.
4 Ball BA, Mohammed HO. Morphometry of stallion spermatozoa by computer-assisted image-analysis. *Theriogenology* 1995; 44: 367–77.
5 Yániz JL, Vicente-Fiel S, Capistrós S, Palacín I, Santolaria P. Automatic evaluation of ram sperm morphometry. *Theriogenology* 2012; 77: 1343–50.
6 Vicente-Fiel S, Palacin I, Santolaria P, Yaniz JL. A comparative study of sperm morphometric subpopulations in cattle, goat, sheep and pigs using a computer-assisted fluorescence method (CASMA-F). *Anim Reprod Sci* 2013; 139: 182–9.
7 Marco-Jimenez F, Viudes-de-Castro MP, Balasch S, Moce E, Silvestre MA, *et al*. Morphometric changes in goat sperm heads induced by cryopreservation. *Cryobiology* 2006; 52: 295–304.
8 Marco-Jimenez F, Vicente JS, Lavara R, Balasch S, Viudes-de-Castro MP. Poor prediction value of sperm head morphometry for fertility and litter size in rabbit. *Reprod Domest Anim* 2010; 45: E118–23.
9 Lavara R, Vicente JS, Baselga M. Genetic variation in head morphometry of rabbit sperm. *Theriogenology* 2013; 80: 313–8.
10 Soler C, Cooper TG, Valverde A, Yaniz JL. Afterword to sperm morphometrics today and tomorrow special issue in *Asian Journal of Andrology*. *Asian J Androl* 2016; 18: 895–7.
11 Soler C, Garcia-Molina A, Contell J, Silvestre MA, Sancho M. The Trumorph® system: the new universal technique for the observation and analysis of the morphology of living sperm. *Anim Reprod Sci* 2015; 158: 1–10.
12 Yaniz JL, Soler C, Alquezar-Baeta C, Santolaria P. Toward an integrative and predictive sperm quality analysis in *Bos taurus*. *Anim Reprod Sci* 2017; 181: 108–14.
13 Palacin I, Vicente-Fiel S, Santolaria P, Yaniz JL. Standardization of CASA sperm motility assessment in the ram. *Small Rum Res* 2013; 112: 128–35.
14 Yaniz JL, Palacin I, Vicente-Fiel S, Gosalvez J, Lopez-Fernandez C, *et al*. Comparison of membrane-permeant fluorescent probes for sperm viability assessment in the ram. *Reprod Domest Anim* 2013; 48: 598–603.
15 Ostermeier GC, Sargeant GA, Yandell BS, Evenson DP, Parrish JJ. Relationship of bull fertility to sperm nuclear shape. *J Androl* 2001; 22: 595–603.
16 Nunez-Martinez I, Moran JM, Pena FJ. Do computer-assisted, morphometric-derived sperm characteristics reflect DNA status in canine spermatozoa? *Reprod Domest Anim* 2005; 40: 537–43.
17 Ostermeier GC, Sargeant GA, Yandell BS, Parrish JJ. Measurement of bovine sperm nuclear shape using Fourier harmonic amplitudes. *J Androl* 2001; 22: 584–94.
18 Yaniz JL, Capistros S, Vicente-Fiel S, Soler C, Nunez de Murga M, *et al*. Use of Relief Contrast® objective to improve sperm morphometric analysis by Isas® casa system in the ram. *Reprod Domest Anim* 2013; 48: 1019–24.
19 Yaniz JL, Capistros S, Vicente-Fiel S, Hidalgo CO, Santolaria P. A comparative study of the morphometry of sperm head components in cattle, sheep, and pigs with a computer-assisted fluorescence method. *Asian J Androl* 2016; 18: 840–3.
20 Yaniz JL, Capistros S, Vicente-Fiel S, Soler C, Nunez de Murga J, *et al*. Study of nuclear and acrosomal sperm morphometry in ram using a computer-assisted sperm morphometry analysis fluorescence (CASMA-F) method. *Theriogenology* 2014; 82: 921–4.
21 Menkveld R, Rhemrev JP, Franken DR, Vermeiden JP, Kruger TF. Acrosomal morphology as a novel criterion for male fertility diagnosis: relation with acrosin activity, morphology (strict criteria), and fertilization *in vitro*. *Fertil Steril* 1996; 65: 637–44.
22 Menkveld R, El-Garem Y, Schill WB, Henkel R. Relationship between human sperm morphology and acrosomal function. *J Assist Reprod Genet* 2003; 20: 432–8.
23 Sailer BL, Jost LK, Evenson DP. Bull sperm head morphometry related to abnormal chromatin structure and fertility. *Cytometry* 1996; 24: 167–73.
24 Lopez-Fernandez C, Fernandez JL, Gosalbez A, Arroyo F, Vazquez JM, *et al*. Dynamics of sperm DNA fragmentation in domestic animals – III. Ram. *Theriogenology* 2008; 70: 898–908.
25 Ramon M, Josefa Soler A, Ortiz JA, Garcia-Alvarez O, Maroto-Morales A, *et al*. Sperm population structure and male fertility: an intraspecific study of sperm design and velocity in red deer. *Biol Reprod* 2013; 89: 110, 1–7.
26 Yaniz JL, Palacin I, Vicente-Fiel S, Sanchez-Nadal JA, Santolaria P. Sperm population structure in high and low field fertility rams. *Anim Reprod Sci* 2015; 156: 128–34.
27 Alquezar-Baeta C, Gimeno-Martos S, Miguel-Jimenez S, Santolaria P, Yaniz J, *et al*. OpenCASA: a new open-source and scalable tool for sperm quality analysis. *Plos Comput Biol* 2019; 15: e1006691.